Laboratory Assessment and Durability Performance of Vinyl-Ester, Polyester, and Epoxy Glass-FRP Bars for Concrete Structures

Brahim Benmokrane,[1] Ahmed H. Ali,[2] Hamdy M. Mohamed,[3]

Adel ElSafty,[4] and Allan Manalo[5]

[1]**Corresponding author.** Professor of Civil Engineering and Tier-1 Canada Research Chair in Advanced Composite Materials for Civil Structures and NSERC Chair in FRP Reinforcement for Concrete Structures, Department of Civil Engineering, University of Sherbrooke, Quebec, Canada, J1K 2R1, Tel.: 1-819-821-7758.

Brahim.Benmokrane@usherbrooke.ca

[2]PhD candidate

Department of Civil Engineering

University of Sherbrooke, Quebec, Canada

Ahmed.Ali@usherbrooke.ca

[3]Postdoctoral fellow

Department of Civil Engineering

University of Sherbrooke, Quebec, Canada

Hamdy.Mohamed@usherbrooke.ca

[4]Professor

Civil Engineering, College of Computing, Engineering, and Construction, UNF, Jacksonville, FL, USA

Adel.el-safty@unf.edu

[5]Senior Lecturer, Centre for Future Materials, Faculty of Health, Engineering and Sciences, University of Southern Queensland, Toowoomba, Queensland 4350, Australia.
manalo@usq.edu.au

Abstract

In the last decade, noncorrosive glass fiber-reinforced-polymer (GFRP) bars have become more widely accepted as cost-effective alternatives to steel bars in many applications for concrete structures (bridges, parking garages, and water tanks). Also, these reinforcing bars are valuable for temporary concrete structures such as soft-eyes in tunneling works. The cost of the GFRP bars can be optimized considering the type of resin according the application. Yet limited research seems to have investigated the durability of GFRP bars manufactured with different types of resin. In this study, the physical and mechanical properties of GFRP bars made with vinyl-ester, isophthalic polyester, or epoxy resins were evaluated first. The long-term performance of these bars under alkaline exposure simulating a concrete environment was then assessed in accordance with ASTM D7705. The alkaline exposure consisted in immersing the bars in an alkaline solution for 1000, 3000 and 5,000 h at elevated temperature (60ºC) to accelerate the effects. Subsequently, the bar properties were assessed and compared with the values obtained on unconditioned reference specimens. The test results reveal that the vinyl-ester and epoxy GFRP bars had the best physical and mechanical properties and lowest degradation rate after conditioning in alkaline solution, while the polyester GFRP bars evidenced the lowest physical and mechanical properties and exhibited significant degradation of physical and mechanical properties after conditioning.

Keywords: Glass fiber; vinyl ester, polyester, epoxy; fiber-reinforced polymer (FRP); glass FRP (GFRP) rebars; physical and mechanical properties; durability performance; alkaline; accelerated aging; microstructural, concrete structures.

Introduction

Fiber-reinforced-polymer (FRP) bars have been well accepted as internal and external reinforcement for concrete structures (ACI 440.1R [ACI 2015]; Benmokrane et al. 2016a; Ali et al. 2016a; Mohamed et al. 2016). This reinforcing material offers better resistance to environmental agents as well as high stiffness-to-weight and strength-to-weight ratios when compared with conventional construction materials such as steel. Extensive research and development efforts have demonstrated that FRP bars are effective reinforcement in concrete members subject to bending (Maranan et al. 2015), shear (Ali et al. 2013 and 2016b), compression (Maranan et al. 2016), and impact (Goldston et al. 2016). Material specifications and design guidelines (ACI 440.6M [ACI 2008]; CAN/CSA S807 [CSA 2010]) have also been developed to encourage the construction industry to use FRP bars. This has resulted in many demonstration projects and field applications, such as bridges (Benmokrane et al. 2004), parking garages (Benmokrane et al. 2012), water-treatment plants (Mohamed and Benmokrane 2014), bridge barriers (El-Salakawy et al. 2005), concrete pavement (Benmokrane et al. 2008), and jetties (Manalo et al. 2014).

Different types of fibers are used in manufacturing FRP bars such as carbon, glass, aramid, and basalt. Many studies have been carried out on the performance and use of FRP bars made with these different fibers, providing good insight into their physical and mechanical properties as well as their durability characteristics (Kocaoz et al. 2005; Banibayat and Patnaik 2014; Ali et al. 2015; Benmokrane et al. 2016a, b; Li et al. 2015; Abbasi and Hogg 2005;

Alsayed et al. 2012; Al-Salloum et al. 2013; Hassan et al. 2016; Tanks et al. 2016). Glass is the most commonly used fiber type in manufacturing FRP bars due to their relatively low comparative cost (ACI 2015). Similarly, Castro et al. (1998) highlighted the importance of the resin system used in manufacturing FRP bars to achieve the desired mechanical properties and durability characteristics. The resin system is important as it acts as a matrix bonding the fibers together and spreading the load applied to the composite between each of the individual fibers. The resin system also protects the fibers from abrasion and impact damage as well as from severe environmental conditions—such as water, salts, and alkalis—which affect the durability of FRP products (SP System 1998). A deterioration of this interface reduces the transfer of the loads between fibers and thus weakens the composite materials (Almusallam et al. 2013). The interface between the fiber and matrix is a nonhomogeneous region about 1 μm thick. This layer is weakly bonded and most vulnerable to deterioration. The three dominant deterioration mechanisms include matrix osmotic cracking, interfacial debonding, and delamination (Chen et al., 2007). Moisture diffusion into FRP composites could be influenced by the material's anisotropic and heterogeneous character. Along with diffusion into the matrix, wicking through the fiber/matrix interface in the fiber direction could be a predominant mechanism of moisture ingress (Apicella et al., 1982). Nonvisible dissociation between fibers and matrix could lead to rapid losses of interfacial shear strength (Ferrier et al. 2016; Ashbee and Wyatt, 1969). Unfortunately, limited research attention has been paid to the effect of the resin-system type on the physical and mechanical properties as well as the durability characteristics of GFRP bars.

Most of the glass-fiber-reinforced polymer (GFRP) bars available are manufactured with E or ECR glass fibers that are normally wetted with a thermosetting resin such as epoxy or vinyl ester. Numerous studies have investigated FRP bars made with vinyl-ester resin to

90 determine the effect of environmental conditions (water, salts, alkalis) on their physical and
91 mechanical properties (Mouritz et al. 2004; Wang 2005; Zou et al. 2008; Robert et al. 2009;
92 Robert and Benmokrane 2013; Benmokrane et al. 2014, 2015, 2016b, 2016c). Similarly, Soles et
93 al. (1998); Amaro et al. 2013; Ali et al. 2015; and Benmokrane et al. (2016a) are some of the
94 numerous researchers who have investigated the durability performance of FRP bars made with
95 epoxy resins. GFRP bars made with these resin systems are the most commonly used as
96 reinforcement for concrete structures given their high performance and very good durability
97 characteristics. Studies into the behavior of fiber-reinforced isophthalic polyester-resin
98 composites have primarily addressed industrial and nonstructural products such as natural-fiber
99 composites (Manalo et al. 2015). GFRP bars manufactured with isophthalic polyester resin are
100 normally used for temporary structures such as soft-eyes in underground excavations and
101 tunneling works (Schurch and Jost 2006). In these proprietary applications, GFRP-bar durability
102 is not a concern. The key advantage of GFRP bars is the low cost of polyester resin and the fact
103 that GFRP bars can be cut without damaging the drilling equipment's cutter heads. Comparisons
104 performed by some researchers [Ashbee et al, 1967; Ashbee and Wyatt, 1969; Abeysinghe et al.,
105 1982] have indicated that the matrix formed by vinyl ester, which contains many fewer ester
106 units compared to polyester, experiences very little deterioration caused by hydroxyl ions
107 compared to a polyester matrix. As a result, CSA S807 (2010) classifies isophthalic polyester-
108 based GFRP bars as having moderate durability (D2), while classifying epoxy- and vinyl-ester-
109 based GFRP bars as having high durability (D1). Obviously, these classifications were
110 established based on the results obtained by different researchers on GFRP bars manufactured
111 with a specific resin system, i.e., either vinyl esters or epoxies (with very few studies on
112 isophthalic polyesters). Consequently, no sound generalizations can be made. Clearly, a single

approach is needed to confirm that GFRP bars manufactured with different types of resin will have different physical and mechanical properties as well as different durability characteristics, therefore providing for direct comparison of these important properties.

This paper presents an experimental investigation aimed at assessing and comparing the physical and mechanical properties of three different types of GFRP bars made with vinyl-ester, isophthalic polyester, or epoxy resins. The tests findings on the long-term durability of these bars conditioned in an alkaline solution simulating a moist concrete environment at high temperature are also presented. The aim is to further understanding of the various resin options available for GFRP bars and their associated behavioral characteristics, yielding useful information about materials specifications and design standards.

Experimental-Program Outline

This experimental investigation was conducted on three different GFRP bars that were 12 mm in diameter: glass/polyester, glass/vinyl-ester, and glass/epoxy as shown in Figure 1. The experimental work was divided into three phases. Phase I included the determination of physical properties, which were compared to those obtained after conditioning. Phase II included mechanical characterization, including transverse shear strength, flexural strength, flexural modulus of elasticity (stiffness), and apparent horizontal shear strength (interlaminar-shear strength). The test results also served as references for residual strength after conditioning. Phase III included a preliminary durability assessment and long-term performance assessment of the GFRP bars immersed in alkaline solutions simulating concrete pore solution at 60°C for different times up to 5,000 h. The changes in the physical and mechanical characteristics were assessed by comparing the characteristics of the conditioned bars to those of the reference bars from Phases I and II. The effects of conditioning on the glass transition temperature (T_g) and chemical

composition of the materials were also assessed with differential scanning calorimetry (DSC) and Fourier transform infrared spectroscopy (FTIR), respectively. In addition, bar microstructure was investigated using scanning electron microscopy (SEM) for both conditioned and unconditioned bars to assess changes and/or degradation.

Material Properties and Test Specimens

The glass/polyester, glass/vinyl-ester, and glass/epoxy FRP bars were manufactured with continuous glass fibers impregnated in polyester, vinyl-ester, or epoxy resins using the pultrusion process. Table 1 lists the typical properties of these thermosetting-resin systems as reported by Bank (2006). The three types of GFRP bars (Figure1) were manufactured by Firep International AG (Switzerland) using the same fabrication process and equipment, same glass fiber, and same additives to ensure bar consistency. The GFRP bars had a nominal diameter of 12 mm and were deformed with helical wrapping (Fig. 1). The nominal cross-sectional area of the three GFRP bars was 113 mm^2, as reported by the manufacturer. The mechanical properties reported herein were calculated using the nominal cross-sectional area.

For this study, the GFRP bars were provided in 170 and 240 mm lengths so that the transverse shear-strength test and flexural test could be performed according to ASTM D7617 (ASTM 2011), and ASTM D4476 (ASTM 2009), respectively. In addition, some specimens were cut into 83 mm lengths so that the short-beam shear test could be performed according to ASTM D4475 (ASTM 2008) on the three types of GFRP bars.

Testing, Results, and Discussion

Phase I: Physical Characterization

Physical properties for the reference (unconditioned) GFRP bars were determined according to ACI (2008) and CSA (2010) requirements, including: (1) fiber content, (2) moisture absorption, (3) cure ratio, and (4) glass transition temperature.

Fiber content

Glass fiber content was determined by thermogravimetry according to ASTM E1131. A very small piece of material (a few tenths milligrams) was cut from the center of the bar, placed in platinum crucible and then heated up to 550°C under inert atmosphere. The weight loss (W_L) has been recorded at a temperature equal to 550°C. Since the material only contains carbon fibers and resin, fiber content by weight was then calculated according to the following equation:

$$\text{Fiber content by weight} = 100 \cdot (W_T - W_L)/W_T \quad (1)$$

where, W_T is the total weight before burn off.

Water-immersion test

The moisture uptake at saturation of the GFRP bars was determined according to ASTM D570, except that the immersion was in tap water instead of distilled water. Three 50 mm long specimens were cut, dried, and weighed prior to immersion in water at 50°C for three weeks. The samples were removed from the water after three weeks, surface dried, and weighed.

The water content at saturation in weight percent (W_s) was calculated using Equation 2

$$W_s = 100 \cdot (P_s - P_d)/P_d \quad (2)$$

where P_s and P_d are the sample weights in the saturated and dry states, respectively.

Cure ratio

Cure ratio was determined according to ASTM D5028 and CSA (2010). The enthalpy of polymerization of the sample was measured by DSC and compared to the enthalpy of polymerization of pure resin, taking into account the weight percentage of resin in the matrix.

Thirty to fifty milligrams of sample were accurately weighed and placed in an aluminum crucible. The samples were then heated from room temperature to 200°C at a heating rate of 20°C/min, and the area of the peak of polymerization was calculated. The measurement was carried out on 3 specimens.

Transverse coefficient of thermal expansion

The transverse coefficient of thermal expansion was calculated according to ASTM E1131-08 (2014). Nine specimens of each type of GFRP bars were tested. The measurements were conducted between -30°C and 60°C at a heating rate of 3°C. A TA Q400 thermomechanical analyzer was used. Cryogenic equipment (liquid nitrogen) was used to reach subzero temperatures. The results show that the coefficients of thermal expansion for the different bar diameters fell between 20.5×10^{-6}/°C and 22.0×10^{-6}/°C, which is only half of the limit of 40.0×10^{-6}/°C specified in CSA 807 (2010).

Table 2 lists the physical properties of the unconditioned GFRP bars, where the glass transition temperature (T_g) was determined with differential scanning calorimetry (DSC) [ASTM D3418 (ASTM 2012b)] (see Fig. 2).

As shown in Table 1, the glass/polyester and glass/epoxy FRP bars had approximately the same fiber content (78.8% and 79.4% by weight, respectively), while the glass/vinyl-ester FRP had the highest fiber–content ratio (83.9% by weight). The average cure ratios and transverse coefficients of thermal expansion of the tested bars were around 99.0±1.0 and $19.25 \pm 1.55 \times 10^{-6}$°C^{-1}, respectively, without significant differences between the three types of bars tested. On the other hand, significant differences were observed for T_g and moisture uptake. The vinyl-ester and polyester GFRP bars returned T_g values of 113°C and 93.0°C, respectively, while the epoxy GFRP bars had a T_g value of 126°C. Similarly, the vinyl-ester and polyester

GFRP bars had water uptake ratios of 0.63% and 1.15%, respectively, while the epoxy GFRP bars had a moisture–uptake ratio of 0.23%. The limits of water absorption of the bars at saturation were <1% and <0.75% for high and medium durability, respectively, as recommended in CSA S807 (2010). The measured water absorption of the polyester GFRP bars was slightly higher than these limits, probably due to the resin-rich deformation pattern on the bar surface, which absorbed most of the moisture.

Phase II: Mechanical Characterization

The mechanical characterization included testing of representative GFRP bars to determine their transverse shear strength in accordance with ASTM D7617 (ASTM 2011); interlaminar shear (short-beam test) in accordance with ASTM D4475 (ASTM 2008); and flexural strength and flexural modulus of elasticity in accordance with ASTM D4476 (ASTM 2009). These tests were selected as they are primarily related to resin properties and can provide a comparative performance assessment of the three GFRP bars tested herein. Figures 3–5 show the mechanical characterization tests and Table 3 lists the results. The following sections provide brief descriptions and interpretation of the results.

Transverse–Shear Strength Test

Transverse shear is the major structural force on dowels in jointed pavements or on stirrups in concrete beams. Transverse-shear tests were conducted according to ASTM D7617 (ASTM 2011) to characterize the tested bars. The setup consisted of a 230 × 100 × 110 mm steel base equipped with lower blades spaced at 50 mm face to face, allowing for the double transverse-shear failure of the specimen caused by an upper blade, as shown in Fig. 3. For each type of bar tested, six unconditioned specimens measuring 170 mm in length were tested under laboratory conditions on an MTS 810 (MTS Systems Corporation, Eden Prairie, Minneapolis) testing

machine equipped with a 500 kN load cell. A displacement-controlled rate of 1.3 mm/min was used during the test, which yielded between 30 and 60 MPa/min until specimen failure. The loading was done without subjecting the test specimens to any shock. The transverse-shear strength was calculated with Eq. (1)

$$\tau_u = \frac{P_s}{2A} \quad (1)$$

where τ_u = transverse-shear strength (MPa); P_s = failure load (N); and A = bar cross-sectional area (mm^2).

Table 3 shows that the transverse-shear strengths of the polyester and vinyl-ester GFRP bars were 250±33 and 258±32 MPa, respectively. The epoxy GFRP bars had the highest value of transverse-shear strength (270±45 MPa). It is worth mentioning, however, that, although the resin delivers most of the transverse-shear strength, the fiber and the fiber/resin interface also play a role (Montaigu et al. 2013). The ratios between the shear strengths of the polyester and vinyl-ester GFRP bars and that of epoxy bars were 93% and 96%, respectively. The results indicate that the epoxy resin yielded higher transverse-shear strength than the polyester and vinyl-ester resin, although the standard deviation was high. Moreover, these values meet CSA requirements (2010), which specify a minimum transverse-shear strength of 160 MPa for GFRP bars.

Three-Point Flexural Test

Flexural testing is especially useful for quality control and specification purposes. Flexural properties may vary with specimen diameter, temperature, weather conditions, and differences in rates of straining. The flexural properties obtained with this test method—ASTM D4476 (ASTM 2009)—cannot be used for design purposes but are appropriate for the comparative testing of composite materials. The test was conducted on specimens 240 mm long over a simply

supported span equal to 20 times the bar diameter, as shown in Fig. 4. Six unconditioned specimens were tested under laboratory conditions as references for each type on an MTS 810 testing machine equipped with a 500 kN load cell. The specimens were loaded at mid-span with a circular nose; the specimen ends rested on two circular supports that allowed the specimens to bend. A displacement-controlled rate of 3.0 mm/min was used during the test. The rate of loading was done without subjecting the test specimen to any shock. The applied load and deflection were recorded during the test on a data-acquisition system monitored by a computer.

The flexural strength of tested FRP specimens was calculated with Eq. (2). The flexural modulus of elasticity (stiffness) is the ratio, within the elastic limit, of stress to corresponding strain. It was calculated with Eq. (3)

$$f_u = PLC / (4I) \quad (2)$$

$$E = PL^3 / (48IY) \quad (3)$$

where f_u = flexural strength in the outer fibers at mid-span (N/mm^2); P = failure load (N); L = clear span (mm); I = moment of inertia (mm^4); C = distance from the centroid to the extremities (mm); E = flexural modulus of elasticity in bending (N/mm^2); and Y = mid-span deflection at load P (mm).

The maximum outer fiber strain (ε_u) was calculated from Eq. (4)

$$\varepsilon_u = f_u / E \quad (4)$$

Table 3 provides the three-point flexural strength, flexural modulus of elasticity, and ultimate outer-fiber strain of the tested GFRP bars. The elastic behavior of all the specimens was maintained until flexural failure, at which point the specimens failed due to compression in the top fibers, as shown in Fig. 4. The polyester GFRP bars showed the lowest flexural strength (1150±59 MPa), while the epoxy GFRP bars recorded the highest (1573±135 MPa). The vinyl-

ester GFRP bars recorded a flexural strength of 1432±75 MPa. The vinyl-ester and epoxy GFRP bars, however, evidenced no significant differences in flexural modulus of elasticity (66.3 and 61.8 GPa, respectively). Lastly, the flexural modulus of elasticity of the polyester resin was lower than that of the vinyl-ester and epoxy resin (86% and 92% of the vinyl-ester and epoxy GFRP bars, respectively). The lower flexural strength and modulus of the polyester GFRP bars is expected since the polyester had the lowest mechanical properties of the thermosetting resins considered (Table 1). Castro and Carino (1998) pointed out that the resin system significantly affected the mechanical properties of FRP bars due to the efficiency of the stress transfer among the fibers.

Short-Beam Shear Test

In FRP bars manufactured with a pultrusion process in which the fibers are arranged unidirectionally and bonded with the polymer matrix, the horizontal stresses would be more conducive to inducing interface degradation than transverse-shear stresses (Park et al. 2008). The short-beam shear test was conducted according to ASTM D4475 (ASTM 2008) on six specimens of each type of GFRP bar in order to calculate the interlaminar-shear strength, which is governed by the fiber–matrix interface. The tests were carried out with a 500 kN MTS 810 testing machine. The distance between the shear planes was set to 7 times the nominal diameter of the FRP bars. Figure 5 shows the test setup and typical modes of failure of the tested specimens. A displacement-controlled rate of 1.3 mm/min was employed during the test. The applied load was recorded with a computer-monitored data-acquisition system.

The interlaminar-shear strength, Su, of the GFRP bars was calculated from Eq. (5)

293 $$S_u = 0.849P / d^2 \quad (5)$$

294 where S_u = interlaminar-shear strength (MPa); P = shear failure load (N); and d = bar diameter
295 (mm).

296 The short-beam shear test revealed that the epoxy GFRP bars had the highest interlaminar-shear
297 strength (77.4±2.7 MPa), followed by the vinyl-ester GFRP bars (64.8±4.5 MPa) and the
298 polyester GFRP bars (47.2±0.4 MPa). The results confirm that the interface between the glass
299 fibers and polyester resin was not as strong as that within the vinyl-ester and epoxy GFRP bars.
300 Table 3 shows the apparent horizontal shear strength of the tested GFRP bars. It is worth
301 mentioning that the high values of the interlaminar-shear strength reveal a strong interface
302 between the resins and reinforcing fibers, which will be clarified in the SEM analysis to follow.

303 **Phase III: Durability Study in Alkaline Solution**

304 **Conditioning of the GFRP Bars in Alkaline Solution**

305 Accelerated aging tests were conducted in accordance with ASTM D7705 (ASTM 2012a). The
306 conditioning of the bars included the combined exposure to a harsh alkaline environment and
307 elevated temperature. Immersion in an aqueous media (alkaline solution) at high temperature
308 accelerates degradation. The alkaline solution was prepared with calcium hydroxide, potassium
309 hydroxide, and sodium hydroxide (118.5 g of $Ca(OH)_2$ + 0.9 g of NaOH + 4.2 g of KOH in 1 L
310 of deionized water) according to ASTM D7705 and CSA S806 (CSA 2012) . The pH of the
311 alkali solution was 12.8. The three types of FRP bars—glass/polyester, glass/vinyl-ester, and
312 glass/epoxy—were immersed in this solution at 60°C for up to 5,000 h. The timing of
313 conditioning started once the solution had reached the prescribed temperature. Robert et al.
314 (2009) reported that the degradation reaction rate increased almost linearly between room
315 temperature and 50°C, whereas the increase was exponential at higher temperatures (over 60°C).

316 Therefore, to avoid any thermal degradation, the maximum conditioning temperature used in this
317 study was 60°C, as specified in ASTM D7705 (ASTM 2012a).
318 The GFRP specimens were placed in hermetically sealed stainless-steel containers to prevent
319 excessive evaporation and the reaction of atmospheric CO_2 with calcium hydroxide. The
320 containers were placed in an environmental chamber adjusted to the prescribed temperature
321 (60°C) under isothermal conditions. The bars were weighed and their diameters measured
322 throughout the conditioning period to monitor water absorption and eventually characterize the
323 mass and diameter changes. Observation revealed no changes in diameter during conditioning.
324 Six specimens of each type of FRP bar were removed from the solution and tested to determine
325 their transverse-shear strength, interlaminar-shear strength, flexural properties, and physical
326 properties after 1,000, 3,000, and 5,000 h at 60°C. Durability was assessed using tests for
327 transverse-shear strength [ASTM D7617 (ASTM2011)], interlaminate shear (short-beam test)
328 [ASTM D4475 (ASTM 2008)], flexural strength, and flexural modulus of elasticity
329 [ASTMD4476 (ASTM 2009)]. Degradation mechanisms in FRP bars are typically denoted as
330 (1) fiber dominated; (2) matrix dominated; and (3) fiber–matrix interface dominated or combined
331 mechanisms. Changes in mechanical properties determined by these tests are indicators of the
332 three specific modes of degradation of the FRP constituent materials given earlier: fibers
333 (flexural tests), resin (transverse and short-beam shear tests), and interface region (short-beam
334 shear and flexural tests). The results for the conditioned specimens were compared to those of
335 the reference ones.

336 **Transverse-Shear Strength of the Conditioned GFRP Bars**

337 Table 4 shows the transverse-shear strength and strength-retention ratios of the tested bars after
338 1,000, 3,000, and 5,000 h of immersion in the alkaline solution at 60°C. Table 4 indicates that

the polyester GFRP bars were highly affected by accelerated aging with a transverse-shear strength reduction of 22.5% after 5,000 h of immersion, while the vinyl-ester and epoxy bars had transverse-shear strength reductions of 15.9% and 11%, respectively. Figure 6(a) shows the effect of the alkaline solution on the transverse shear strength after different exposure times. Contrary to the polyester bars, the vinyl-ester and epoxy GFRP bars exhibited no significant reductions in the early stages (less than 3,000 h).

Flexural Strength of the Conditioned FRP Bars

Table 4 provides the flexural strength and strength-retention ratios of the tested FRP bars after 1,000, 3,000, and 5,000 h of immersion. Both the polyester and epoxy GFRP bars had similar flexural-strength reductions after 5,000 h (25 and 23%, respectively), while the vinyl-ester GFRP bars showed a lower reduction of 17%. These observations confirm that the bond between the GFRP fibers and polyester resin—before and after conditioning—was lower than that between the glass fibers in the vinyl-ester or epoxy resin. Consequently, debonding occurring at the fiber–matrix interface caused the fibers to separate from the resin. Figure 6(b) shows the effect of the alkaline solution on flexural strength. The lowest reduction rate was observed with the vinyl-ester GFRP bars, which yielded the lowest degradation at the interface. The high degradation of the epoxy GFRP bars after 1,000 h of conditioning resulted from the ingress of the alkaline solution through the initial voids. The polyester GFRP bars, however, returned an almost steady degradation rate between 1,000 and 5,000 h.

Flexural Modulus of Elasticity of the Conditioned GFRP Bars

Table 4 gives the flexural modulus of elasticity and the retention ratio of the tested FRP bars after 1,000, 3,000, and 5,000 h of immersion. The three bar types had no significant differences in flexural modulus of elasticity after 5,000 h. The reduction ranged from 10.7% to 12.6% in

362 comparison to the references. Figure 6(c) illustrates the effect of the alkaline solution on the
363 flexural modulus of elasticity, with all types of bar specimens exhibiting a steady reduction rate.

364 **Interlaminar-shear strength of the Conditioned GFRP Bars**

365 Table 4 also shows the apparent horizontal shear (interlaminar shear) strength and strength-
366 retention ratios of the tested FRP bars after 1,000, 3,000, and 5,000 h of immersion. As for
367 flexural testing, the vinyl-ester and epoxy GFRP bars offered excellent stability and durability
368 after immersion in the alkaline solution, followed by the polyester GFRP bars. The reduction
369 ratios for the vinyl-ester, epoxy, and polyester GFRP bars after 5,000 h were 13%, 13%, and
370 21%, respectively. Again, this observation confirms the strong fiber–resin interface in the vinyl-
371 ester GFRP bars, followed by the epoxy and polyester GFRP bars. As evidenced from these
372 results, the fiber–resin interface stands out as one of the most important issues in manufacturing
373 glass FRP. Figure 6(d) shows the effect of the alkaline solution on the interlaminar-shear
374 strength, with the vinyl-ester GFRP bars exhibiting the lowest rate of degradation. Interestingly,
375 the 21% reduction in the interlaminar-shear strength of the polyester GFRP bars in this study is
376 significantly lower than with the polyester E-glass composite rods tested by Micelli and Nanni
377 (2004), who observed a more than 90% reduction in interlaminar-shear strength. This indicates
378 that the development of new material systems and advanced manufacturing methods now yield
379 high-quality FRP bar products.

380 **Microstructural Analysis of the Reference and Conditioned GFRP Bars**

381 SEM observations were performed to investigate microstructural changes in the GFRP bars
382 before and after conditioning. The specimens were cut, polished, and coated with a thin layer of
383 gold/palladium in a vapor-deposit process. The analysis was carried out on a JEOL JSM-840 A
384 microscope (JEOL, Akishima, Tokyo, Japan). Figure 7 shows the SEM micrographs of the cross

section of the reference GFRP bars, while Figs. 8 to 10 provide the SEM micrographs of the 5,000 h conditioned specimens.

SEM analysis of the reference and conditioned specimens (Figs. 7 to 10) indicates that the GFRP bars made with vinyl-ester and epoxy evidenced no significant changes, but presented a slight debonding at the interface between the fibers and vinyl-ester resin. Consequently, the vinyl-ester GFRP bars evidenced higher moisture uptake measured at saturation compared to the epoxy GFRP bars. On the other hand, the GFRP bars containing the polyester resin evidenced significant impact on the coating with the 5000 h conditioning. Moreover, these bars experienced greater debonding at the fiber–resin interface than did the vinyl-ester and epoxy GFRP bars. Accordingly, the polyester GFRP bars had higher moisture uptake measured at saturation and higher degradation rate of mechanical properties after conditioning.

SEM was also performed on the fracture zones of the 1,000 h specimens after short-beam testing (Fig. 11) to investigate the mechanisms of failure at the interface fiber–matrix. The fiber surface of the vinyl-ester and epoxy GFRP bars had more resin coverage (Fig. 11 [b and c]) than the polyester GFRP bars (Fig. 11[a]). This observation corroborates the reduction ratio of the interlaminar-shear strength and flexural strength after conditioning in the alkaline solution and characterizes the higher bonding of the glass fiber to the vinyl-ester and epoxy resins than the polyester resin.

Glass Transition Temperature and Cure Ratio of the Conditioned GFRP Bars

Differential scanning calorimetry (DSC) is used to obtain information about the thermal behavior and characteristics of polymeric materials and composites, such as the glass transition temperature (T_g) and curing process. In this study, 30–50 mg specimens from both unconditioned and conditioned specimens were sealed in aluminum pans and heated in a TA Instruments (New

Castle, Delaware) DSC Q10 calorimeter to 200°C at a rate of 20°C/min. The glass transition temperature (T_g) was determined in accordance with ASTM D3418 (ASTM 2012b).

Table 5 presents the T_g values for the reference and specimens conditioned for 5,000 h. The T_g of the conditioned polyester GFRP bars were slightly higher than that of the reference specimens, as a result of post-curing at high temperature. The vinyl-ester and epoxy GFRP bars were almost fully cured (99.1% and 100%, respectively); their T_g values were lower than that of the reference specimens by 11.5% and 10.3%, respectively. Epoxy resin is known to lower T_g when water is absorbed (plasticizing effect). The water absorption of the epoxy GFRP bars was 0.2%.

Chemical Changes in the Conditioned GFRP Bars

Fourier transform infrared spectroscopy (FTIR) was used to identify any chemical change/degradation after 5,000 h of conditioning at 60ºC. FTIR spectra of the surface and core of the material specimens were recorded using a Jasco 4600 spectrometer equipped with an attenuated total-reflectance device. Five hundred and twelve scans were routinely acquired at a resolution of 4 cm^{-1}. Chemical degradation in the alkaline solution is mainly due to a hydrolysis reaction, which forms new hydroxyl (-OH) groups from sensitive units, such as ester groups. Hydroxyl groups appeared as a broad peak between 3200 and 3650 cm^{-1}, which corresponds to the stretching mode of the hydroxyl groups in the polyester, vinyl-ester, and epoxy resins.

Figure 12 shows the FTIR spectra of the unconditioned and conditioned polyester, vinyl-ester, and epoxy GFRP specimens conditioned in the alkaline solution for 5,000 h at 60°C. For each specimen—reference and conditioned—spectra of the surface and core of the specimen were recorded and the areas of the O–H and C–H peaks calculated as presented in Fig. 13. Table 6 presents the ratio of the (OH^-) peak to the resin's carbon–hydrogen (C–H) stretching peak. The table indicates that none of the hydroxyl peaks for any of the tested vinyl-ester and epoxy GFRP

specimens evidenced any significant changes, which equates to no increase in the amount of hydroxyl groups in the resins. This observation shows that the vinyl-ester and epoxy resins used did not degrade chemically while the specimens were immersed at 60°C for 5,000 h. On the other hand, the polyester resin showed significant differences on the surface and in the core of the tested specimens (see Table 6). The experimental O–H/C–H for the core and surface of the vinyl-ester and epoxy GFRP bars immersed for 5,000 h were 1.5, 1.8, 1.2, and 1.5, respectively, compared to 1.80, 2.40, 1.25, and 1.6 for the unconditioned specimens, while the experimental ratios for the core and surface of the polyester GFRP bars immersed for 5,000 h at 60°C were 3.5 and 14.30, respectively. These results led to the conclusion that chemical degradation of the polymer occurred on the surface of the polyester bars, which was in direct contact with the solution during immersion. This observation explains the losses in mechanical properties of the polyester GFRP bars.

Moisture Uptake at Saturation of the Conditioned GFRP Bars

The moisture uptake at saturation of the reference and conditioned FRP bars was determined according to ASTM D570 (ASTM 2010). The gain in mass was corrected to account for specimen mass loss due to possible dissolution phenomena. This correction was achieved by completely drying the immersed specimens in an oven at 100°C for 24 h and comparing their masses to their initial masses. The mass loss may have occurred due to several causes: dissolution of soluble chemicals present on the surface; sand debonding in the case of sand-coated bars; and chemical degradation of one of the components, such as resin hydrolysis. In this study, the moisture-uptake ratios at saturation for the reference specimens were 1.15%, 0.63%, and 0.23% for the polyester, vinyl-ester, and epoxy GFRP, respectively, while these ratios for the conditioned specimens were 1.36%, 0.38%, and 0.20% for the polyester, vinyl-ester, and epoxy

GFRP bars, respectively. The epoxy GFRP bars had the lowest water uptake, which is consistent with the lowest degradation of the fiber–resin interface as determined by DSC analysis and SEM observations.

Summary and Conclusions

This study investigated glass-fiber-reinforced polymers (GFRPs) with polyester, vinyl-ester, and epoxy resins. Based on the results, the following conclusions concerning the glass FRP bars made with polyester, vinyl-ester and epoxy resins tested herein can be drawn:

1. The epoxy and vinyl-ester GFRP bars exhibited higher fiber–resin bond; flexural strength; flexural modulus of elasticity; and interlaminar-shear strength, which is governed by the fiber–matrix interface. In addition, they showed lower moisture uptake.

2. Both the polyester and epoxy GFRP bars had similar flexural-strength reductions after 5,000 h of immersion (25% and 23%, respectively), while the vinyl-ester GFRP bars returned a lower reduction of 17%. These observations confirm that the bond between the GFRP fibers and polyester resin—before and after conditioning—was lower than that between the glass fibers and the vinyl-ester or epoxy resin.

3. The unconditioned polyester GFRP bars exhibited lower transverse-shear strength, flexural strength, interlaminar-shear strength, and the weakest fiber–resin interface. The transverse-shear strength of the polyester GFRP bars was significantly affected by accelerated aging (22.5% reduction after 5,000 h), while the epoxy and vinyl-ester GFRP bars were slightly affected by accelerated aging (11% and 15.9 % reductions, respectively, after 5,000 h).

4. The flexural strength of the polyester GFRP bars was significantly affected by accelerated aging (25% reduction after 5,000 h), while the vinyl-ester and epoxy GFRP bars were affected by accelerated aging (17% and 23% reductions, respectively, after 5,000 h).

5. The interlaminar-shear strength of the polyester GFRP bars was highly affected by accelerated aging (21% reduction after 5,000 h), while the vinyl-ester and epoxy GFRP bars were slightly affected by accelerated aging (13% reduction each after 5,000 h). The fiber–resin interface plays a significant role in controlling the degradation due to conditioning.

6. The microstructural observations revealed that GFRP bars made with vinyl-ester or epoxy resin were not significantly changed, but presented a slight debonding at the interface between the fibers and vinyl-ester resin. Consequently, the vinyl-ester GFRP bars evidenced higher moisture uptake measured at saturation compared to the epoxy GFRP bars.

7. The debonding at the interface between the fibers and polyester resin was higher than in the vinyl-ester and epoxy GFRP bars. Accordingly, the polyester GFRP bars evidenced higher moisture uptake measured at saturation and a higher degradation rate of mechanical properties after conditioning.

8. The polyester GFRP bars showed an increase in T_g of about 5°C after conditioning due to post-curing (cure ratio of the reference specimens was 98.1%). The vinyl-ester and epoxy GFRP bars, however, experienced a decrease in T_g after conditioning.

9. The polyester GFRP bars absorbed 18% more water than the vinyl-ester and epoxy GFRP bars after conditioning compared to the reference specimen.

Acknowledgments

The authors wish to acknowledge the financial support of the Natural Sciences and Engineering Research Council of Canada (NSERC), the NSERC Research Chair in Innovative FRP Reinforcement for Concrete Structures, the Fonds de la recherche du Quebec en nature et technologies (FRQ-NT), the Florida Department of Transportation, and the University of North Florida. The authors would like to thank Firep International AG (Switzerland) for donating the GFRP materials and the technical staff of the structural & materials lab in the Department of Civil Engineering at the University of Sherbrooke.

References

Abbasi, A., and Hogg, P. J. (2005). "Temperature and Environmental Effects on Glass Fiber Rebar: Modulus, Strength and Interfacial Bond Strength with Concrete." *Composites Part B: Engineering*, 36(5), 394-404.

Abeysinghe, H., Edwards, W., Pritchard, G., and Swampillai, G., J. (1982). "Degradation of crosslinked resins in water and electrolyte solutions." *Polymer*, 23(12), 1785–1790.

ACI (American Concrete Institute). (2008). "Specification for carbon and glass fiber-reinforced polymer bar materials for concrete reinforcement." *ACI 440.6M-08*, Farmington Hills, MI.

ACI (American Concrete Institute). (2015). "Guide for the design and construction of structural concrete reinforced with FRP bars." *ACI 440.1R-15*, Farmington Hills, MI.

Ali, A. H., Mohamed, H. M., and Benmokrane, B. (2013). "Shear resistance of circular concrete members reinforced with FRP bars: Code predictions and numerical analysis." *Proc., CSCE Annual Conf., Canadian Society for Civil Engineering* (CSCE), Montreal.

516 Ali, A. H., Mohamed, H. M., and Benmokrane, B. (2016a). "Shear behavior of circular concrete
517 members reinforced with GFRP bars and spirals at shear span-to-depth ratios between 1.5 and
518 3.0." *J. Compos. Constr*., 10.1061/(ASCE)CC.1943-5614.0000707, 04016055.
519 Ali, A. H., Mohamed, H. M., and Benmokrane, B. (2016b). "Strength and Behavior of Circular
520 FRP-Reinforced Concrete Sections without Web Reinforcement in Shear." *J. Struct.*
521 *Eng.*, 10.1061/(ASCE)ST.1943-541X.0001684 , 04016196.
522 Ali, A. H., Mohamed, H. M., ElSafty, A., and Benmokrane, B. (2015). "Long-term durability
523 testing of Tokyo rope carbon cables." *20th International Conference on Composite Materials*,
524 (ICCM20), Copenhagen, Denmark, 19-24th July, 2015.
525 Almusallam, T. H., Al-Salloum, Y.A., Alsayed, S., H., El-Gamal, S., and Aqel, M. (2013).
526 "Tensile properties of glass fiber-reinforced polymer bars embedded in concrete under severe
527 laboratory and field environmental conditions." *J. Compos. Mater.*, 47(4), 393-407.
528 Al-Salloum, Y., El-Gamal, S., Almusallam, T., Alsayed, S., and Aqel, M. (2013). "Effect of
529 harsh environmental conditions on the tensile properties of GFRP bars." *Composites Part B:*
530 *Engineering, 45(1), 835–844.*
531 Alsayed, S., Al-Salloum, Y., Almusallam, T., El-Gamal, S., and Aqel, M. (2012).
532 "Performance of glass fiber reinforced polymer bars under elevated temperatures." *Composites*
533 *Part B : Engineering, 43, 2265-2271*.
534 Amaro, A.M., Reis, P.N.B., Neto, M.A., and Louro, C. (2013). "Effects of Alkaline and Acid
535 Solutions on Glass/Epoxy Composites." *Polymer Degradation and Stability, 98(4), 853-862.*
536

Apicella A., Migliaresi C., Nicodemo L., Nicolais L., Iaccarino L., and Roccotelli S. (1982). "Water sorption and mechanical properties of a glass-reinforced polyester resin." *Composites, 13(4), 406–410*.

Ashbee, K., and Wyatt, R. (1969). "Water damage in glass fibre/resin composites." *Proc. Roy. Soc. Lond, Ser. A*, 312(1511), 553–564.

Ashbee, K., Frank F., and Wyatt, R. (1967). "Water damage in polyester resins." Proc. Roy. Soc. Lond, Ser. A, 300(1463), 415–419.

ASTM. (2008). "Standard test method for apparent horizontal shear strength of pultruded reinforced plastic rods by the short beam method." *ASTM D4475*, West Conshohocken, PA.

ASTM. (2009). "Standard test method for flexural properties of fiber reinforced pultruded plastic rods." ASTM D4476, West Conshohocken, PA.

ASTM. (2010). "Water absorption of plastics." *ASTM D570*, West Conshohocken, PA.

ASTM. (2011). "Standard test method for transverse shear strength of fiber-reinforced polymer matrix composite bars." *ASTM D7617*, West Conshohocken, PA.

ASTM. (2012a). "Standard test method for alkali resistance of fiber reinforced polymer (FRP) matrix composite bars used in concrete construction." *ASTM D7705*, West Conshohocken, PA.

ASTM. (2012b). "Standard test method for transition temperatures and enthalpies of fusion and crystallization of polymers by differential scanning calorimetry." *ASTM D3418*, West Conshohocken, PA.

Banibayat, P., and Patnaik, A. (2014). "Variability of mechanical properties of basalt fiber reinforced polymer bars manufactured by wet lay-up method." *Materials and Design*, 56, 898–906.

559 Bank, L. C. (2006). “Composites for Construction: Structural Design with FRP Materials.”
560 Wiley, Hoboken, DOI: 10.1002/9780470121429.
561 Benmokrane, B. Ali, A. H., Mohamed, H. M. and Safty, A. (2014). “Long-Term Tensile
562 Properties of Carbon FRP Cable.” *15th International European Bridge Conference*, London, UK
563 8-10th, July 2014.
564 Benmokrane, B., Ahmed, E., Dulude, C., and Boucher, E. (2012). “Design, construction, and
565 monitoring of the first worldwide two-way flat slab parking garage reinforced with GFRP bars.”
566 *Proc., 6th Int. Conf. on FRP Composites in Civil Engineering*, International Institute for FRP in
567 Construction, Kingston, ON, Canada
568 Benmokrane, B., Eisa, M., El-Gamal, S., Thébeau, D., and El-Salakawy, E. (2008). “Pavement
569 system suiting local conditions: Québec studies continuously reinforced concrete pavement with
570 glass fiber-reinforced polymer bars.” *J. Am. Concr. Inst.*, 30(11), 34–39.
571 Benmokrane, B., El-Salakawy, E., Desgagné, G., and Lackey, T. (2004). “FRP bars for bridges.”
572 Concr. Int., 26(8), 84–90.
573 Benmokrane, B., Ali, A. H., Mohamed, H.M., Robert, M., and ElSafty, A. (2016a). “Durability
574 Performance and Service Life of CFCC Tendons Exposed to Elevated Temperature and Alkaline
575 Environment.” *J. Compos. Constr.*, 10.1061/(ASCE)CC.1943-5614.0000606, 04015043.
576 Benmokrane, B., Mohamed, H., Manalo, A., and Cousin, P. (2016c). “Evaluation of Physical and
577 Durability Characteristics of New Headed Glass Fiber–Reinforced Polymer Bars for Concrete
578 Structures.” *J. Compos. Constr.*, 10.1061/(ASCE)CC.1943-5614.0000738, 04016081.
579 Benmokrane, B., Elgabbas, F., Ahmed, E., and Cousin, P. (2015). “Characterization and
580 Comparative Durability Study of Glass/Vinylester, Basalt/Vinylester, and Basalt/Epoxy FRP
581 Bars.” *J. Compos. Constr.*, 10.1061/(ASCE)CC.1943-5614.0000564, 04015008.

582 Benmokrane, B., Robert, M., Mohamed, H., Ali, A. H., and Cousin, P. (2016b). "Durability
583 Assessment of Glass FRP Solid and Hollow Bars (Rock Bolts) for Application in Ground
584 Control of Jurong Rock Caverns in Singapore." *J. Compos. Constr*., 10.1061/(ASCE)CC.1943-
585 5614.0000775, 06016002.
586 Canadian Standards Association (CSA). (2010). "Specification for fibre reinforced polymers."
587 *CAN/CSA S807-10*, Rexdale, Ontario, Canada.
588 Canadian Standards Association (CSA). (2012). "Design and construction of building
589 components with fibre-reinforced polymers." *CAN/CSA S806-12*, Rexdale, Ontario, Canada.
590 Castro, P.F. and Carino, N.J. (1998) "Tensile and non-destructive testing of FRP bars." *J.*
591 *Compos. Constr.*, 2(1), 17-27.
592 Chen, Y., Davalos, J.F., Ray, I. and Kim, H.Y. (2007). "Accelerated Aging Tests for Evaluation
593 of Durability Performance of FRP Reinforcing Bars Reinforcing Bars for Concrete Structures."
594 *Composite Structures, 78(1), 101-111.*
595 El-Salakawy, E.F., Benmokrane, B. and Brière, F. (2005). "Glass FRP composite bars for
596 concrete bridge barriers." *Journal of Science and Eng. of Composite Materials*, 12(3), 167-192.
597 Ferrier, E., Rabinovitch, O., and Michel, L. (2016). "Mechanical behavior of concrete
598 resin/adhesive–FRP structural assemblies under low and high temperatures." *Construction and*
599 *Building Materials, 127, 1017-1028.*
600 Goldston, M., Remennikov, A., and Neaz Sheikh, M. (2016). "Experimental investigation of the
601 behavior of concrete beams reinforced with GFRP bars under static and impact loading."
602 *Engineering Structures*, 113, 220-232.

603 Hassan, M., Benmokrane, B., ElSafty, A., and Fam, A. (2016) “Bond durability of basalt-fiber-
604 reinforced-polymer (BFRP) bars embedded in concrete in aggressive environments.” *Composites*
605 *Part B : Engineering, 106, 262-272*.
606 Kocaoz, S., Samaranayake, V.A., and Nanni, A. (2005). “Tensile characterization of glass FRP
607 bars.” *Composites: Part B : Engineering*, 36, 127-134.
608 Li, G., Wu, J., and Ge, W. (2015). “Effect of loading rate and chemical corrosion on the
609 mechanical properties of large diameter glass/basalt-glass FRP bars.” *Construction and Building*
610 *Materials,* 93, 1059-1066.
611 Manalo, A.C., Benmokrane, B., Park, K., and Lutze, D. (2014). “Recent developments on FRP
612 bars as internal reinforcement in concrete structures.” *Concrete in Australia,* 40(2), 46-56.
613 Manalo, A.C., Wani, E., Zukarnain, N.A., Karunasena, K., and Lau, K.T. (2015). “Effects of
614 alkali treatment and elevated temperature on the mechanical properties of bamboo fibre–
615 polyester composites.” *Composites Part B: Engineering, 80, 73–83*.
616 Maranan, G., Manalo, A. C., Benmokrane, B. and Karunasena, W. and Mendis, P. (2015).
617 “Evaluation of the flexural strength and serviceability of geopolymer concrete beams reinforced
618 with glass-fibre-reinforced polymer (GFRP) bars.” *Engineering Structures*, 101, 529-541.
619 Maranan, G.B., Manalo, A.C., Benmokrane, B., Karunasena, W., and Mendis, P. (2016).
620 “Behavior of concentrically loaded geopolymer-concrete columns reinforced longitudinally and
621 transversely with GFRP bars.” *Engineering Structures*, 117, 422–436.
622 Micelli, F., and Nanni, A. (2004). “Durability of FRP rods for concrete structures.” *Construction*
623 *and Building Materials,* 18, 491-503.

624 Mohamed, H. M., and Benmokrane, B. (2014). “Design and performance of reinforced concrete
625 water chlorination tank totally reinforced with GFRP bars: Case study.” *J. Compos. Constr.*,
626 10.1061/(ASCE)CC.1943-5614.0000429, 05013001-1–05013001-11.
627 Mohamed, H. M., Ali, A. H., and Benmokrane, B. (2016). “Behavior of Circular Concrete
628 Members Reinforced with Carbon-FRP Bars and Spirals under Shear.” *J. Compos.*
629 *Constr*., 10.1061/(ASCE)CC.1943-5614.0000746 , 04016090.
630 Montaigu, M., Robert, M., Ahmed, E., and Benmokrane, B. (2013). “Laboratory characterization
631 and evaluation of durability performance of new polyester and vinyl-ester e-glass GFRP dowels
632 for jointed concrete pavement.” *J. Compos. Constr*., 10.1061/(ASCE)CC.1943-5614.0000317,
633 176–187.
634 Mouritz, A. P., Kootsookos, A., and Mathys, G. (2004). “Stability of polyester- and vinyl-ester-
635 based composites in seawater.” *J. Mater. Sci*., 39(19), 6073–6077.
636 Park, C., Jang, C., Lee, S., and Won, J. (2008). “Microstructural investigation of long-term
637 degradation mechanisms in GFRP dowel bars for jointed concrete pavement.” *J. Appl. Polym.*
638 *Sci*., 108(5), 3128–3137.
639 Robert, M., and Benmokrane, B., (2013). “Combined effects of saline solution and moist
640 concrete on long-term durability of GFRP reinforcing bars.” *Construction and Building*
641 *Materials, 38: 274-284.*
642 Robert, M., Cousin, P., and Benmokrane, B. (2009). “Durability of GFRP reinforcing bars
643 embedded in moist concrete.” *J. Compos. Constr*., 10.1061/(ASCE)1090-0268(2009)13:2(66),
644 66–73.

Schurch, M., and Jost, P. (2006). "GFRP soft-eye for TBM Breakthrough: Possibilities with a modern construction material." *Proc. International Symposium on Underground Excavation and Tunnelling*, Bangkok, Thailand, 397-404.

Soles C. L., Chang, F. T., Bolan, B. A., Hristov, H. A., Gidley, D. W., and Yee, A. F. (1998). "Contributions of the nanovoid structure to the moisture absorption properties of epoxy resins." *J Polym. Sci. Part B*: *Poly. Phys*., 36(17), 3035–3048.

SP System. (1998). "Structural polymer system—Composite engineering material." Clause "Guide to Resin Systems for Composites, GTRS-1- 1098", Newport, Isle of Wight, U.K., 1–15.

Tanks, J. D., Harris, D. K., and Sharp, S. R. (2016) "Mechanical response of unidirectional composite bars loaded in transverse compression." *Composites Part B : Engineering, Vol. 97, 18-25.*

Wang, P. (2005). "Effect of moisture, temperature, and alkaline on durability of E-glass/vinyl-ester reinforcing bars." *Ph.D. thesis, Univ. of Sherbrooke*, Sherbrooke, Canada.

Zou, C., Fothergill, J. C., and Rowe, S. W. (2008). "The effect of water absorption on the dielectric properties of epoxy nanocomposites." *IEEE Trans. Dielectr. Electr. Insul*., 15(1), 106–117.

List of Tables

Table 1. Typical properties of the thermosetting resins (Bank, 2006)

Table 2. Physical properties of the reference GFRP bars

Table 3. Mechanical properties of the reference GFRP bars

Table 4. Retention of mechanical properties of the conditioned GFRP bars

Table 5. Cure ratio, T_g, and moisture uptake of the reference and conditioned GFRP bars

Table 6. Ratio of the FTIR peaks

Table 1. Typical properties of the thermosetting resins (Bank, 2006)

Property	Resin system		
	Polyester	Vinyl-ester	Epoxy
Glass transition temperature (Tg), ^{o}C	100	110	120
Tensile modulus, GPa	4.0	3.5	3.0
Tensile strength, MPa	65	82	90
Elongation at break, %	2.5	6.0	8.0

Table 2. Physical properties of the reference GFRP bars

Property	GFRP bar type		
	Polyester	Vinyl-ester	Epoxy
Fiber content by weight (%)	78.8	83.9	79.4
Cure ratio (%)	98.1	99.1	100
Transverse CTE, ($x10^{-6o}C^{-1}$)	20.8	17.7	19.7
Glass transition temperature, Tg (^{o}C)	93.0	113	126
Moisture uptake (%)	1.15	0.63	0.23

Table 3. Mechanical properties of the reference GFRP bars

Bar type	τ_u (MPa)	f_u (MPa)	E (GPa)	ε_u (%)	S_u (MPa)
Glass/polyester	250±33	1150±59	56.9±2.4	2.02±0.16	47.2±0.4
Glass/vinyl-ester	258±32	1432±75	66.3±2.2	2.16±0.089	64.8±4.5
Glass/epoxy	270±45	1573±135	61.8±1.5	2.54±0.015	77.4±2.7

677 **Table 4.** Retention of mechanical properties of the conditioned GFRP bars

Fiber/resin	Conditioned period	τ_u (MPa)	Retention (%)	f_u (MPa)	Retention (%)	E (GPa)	Retention (%)	S_u (MPa)	Retention (%)
Glass/polyester	1,000	236	94.4	1133	99	55.0	96.6	43.8	93
	3,000	222	88.8	939	81	54.0	94.9	40.8	87
	5,000	194	77.5	863	75	50.8	89.3	37.4	79
Glass/vinyl-ester	1,000	248	96.1	1409	98	64.0	96.5	62.5	97
	3,000	234	90.7	1273	89	61.1	92.2	58.0	90
	5,000	217	84.1	1186	83	58.5	88.2	56.0	87
Glass/epoxy	1,000	267	98.9	1446	92	59.0	95.5	73.7	96
	3,000	248	92.0	1301	83	57.5	93.0	69.6	90
	5,000	239	89.0	1211	77	54.0	87.4	67.0	87

678

679 **Table 5.** Cure ratio, T_g, and moisture uptake of the reference and conditioned GFRP bars

Property	GFRP bar type					
	Polyester		Vinyl-ester		Epoxy	
	Reference	5,000 h	Reference	5,000 h	Reference	5,000 h
Cure ratio (%)	98	100	99	99	100	100
Tg (°C)	93	98	113	100	126	112
Moisture uptake (%)	1.15	1.36	0.63	0.38	0.23	0.20

680

681

682 **Table 6.** Ratio of the FTIR peaks

Test location	OH/CH ratio					
	Polyester		Vinyl-ester		Epoxy	
	Reference	5,000 h	Reference	5,000 h	Reference	5,000 h
Surface	2.60	14.3	2.40	1.80	1.60	1.50
Core	1.60	3.50	1.80	1.50	1.25	1.20

683

684

685

686

687 **List of Figures**

688 Figure 1. Tested GFRP bars

689 Figure 2. DSC scans for glass transition temperature (T_g)

690 Figure 3. Setup for transverse-shear test and typical shear failure mode: (a) test setup; (b) failure
691 mode

692 Figure 4. Setup for flexural testing and typical failure mode: (a) test setup; (b) failure mode

693 Figure 5. Setup for short-beam testing and typical failure mode: (a) test setup; (b) failure mode

694 Figure 6. Effect of conditioning in the alkaline solution at 60°C on mechanical properties:
695 (a) transverse-shear strength; (b) flexural strength; (c) flexural modulus of elasticity;
696 (d) interlaminar-shear strength

697 Figure 7. Micrographs of the cross section of the reference FRP bars

698 Figure 8. Micrographs of the fiber/matrix interface of a glass/epoxy bar before and after
699 conditioning: (a) before conditioning; (b) after conditioning

700 Figure 9. Micrographs of the fiber–matrix interface of a glass/polyester bar before and after
701 conditioning: (a) before conditioning; (b) after conditioning

702 Figure 10. Micrographs of the fiber–matrix interface of a glass/vinyl-ester bar before and after
703 conditioning: (a) before conditioning; (b) after conditioning

704 Figure 11. Micrographs of bars conditioned in the alkaline solution for 1,000 h at 60oC (after
705 interlaminar shear failure): (a) glass/epoxy; (b) glass/polyester; (c) glass/vinyl-ester

706 Figure 12. FTIR spectra of reference and specimens conditioned for 5,000 h

707 **Figure 13.** Peak areas used to calculate a O–H/C–H

708

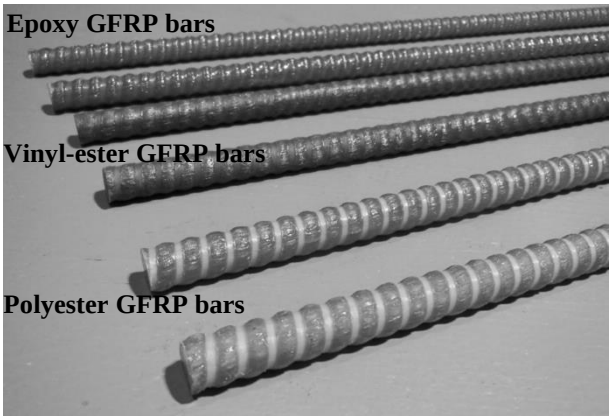

709

710 **Figure 1**. Tested GFRP bars

711

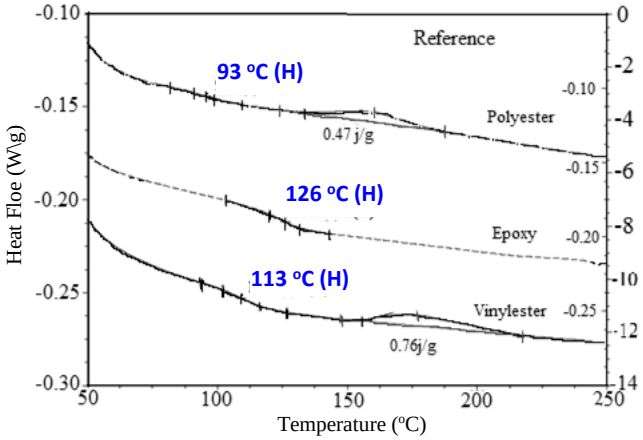

712

713 **Figure 2**. DSC scans for glass transition temperature (T_g)

714

715

716

717

718

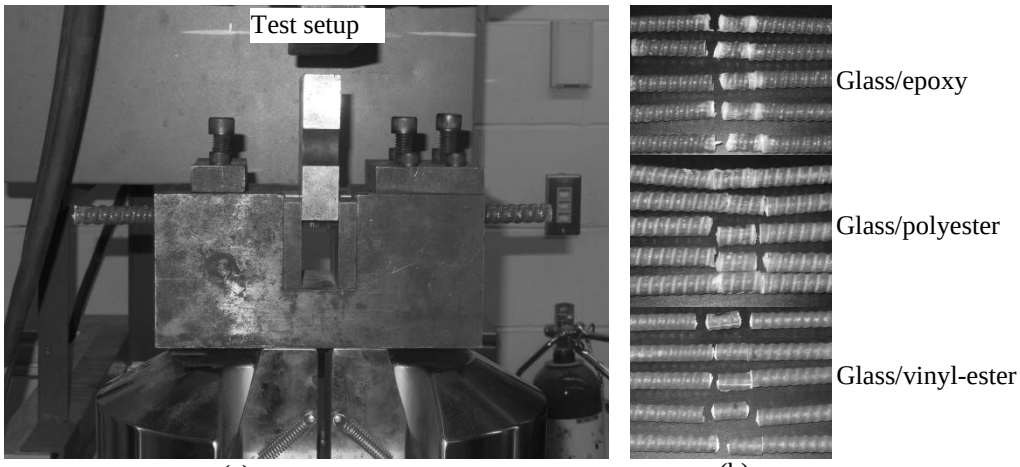

(a) (b)

Figure 3. Setup for transverse-shear test and typical shear failure mode: (a) test setup; (b) failure mode

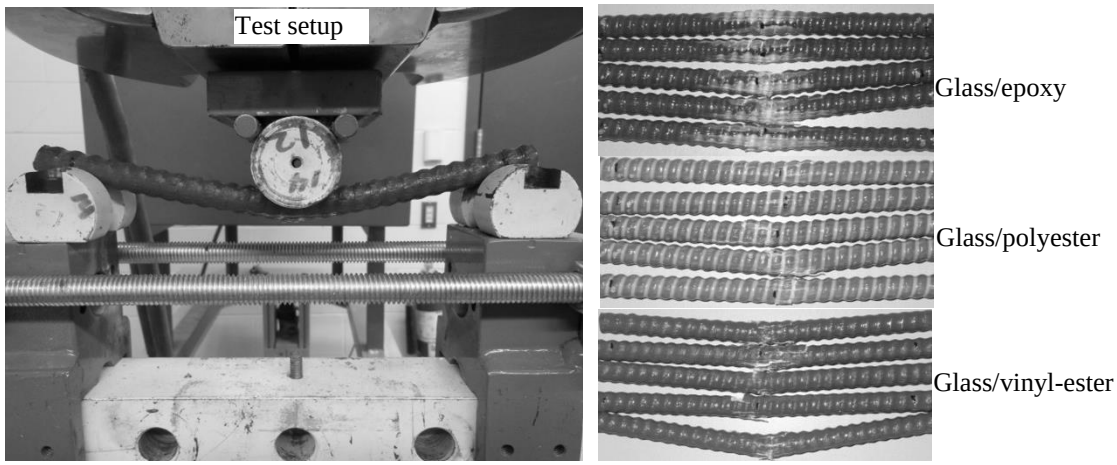

(a) (b)

Figure 4. Setup for flexural testing and typical failure mode: (a) test setup; (b) failure mode

Figure 5. Setup for short-beam testing and typical failure mode: (a) test setup; (b) failure mode

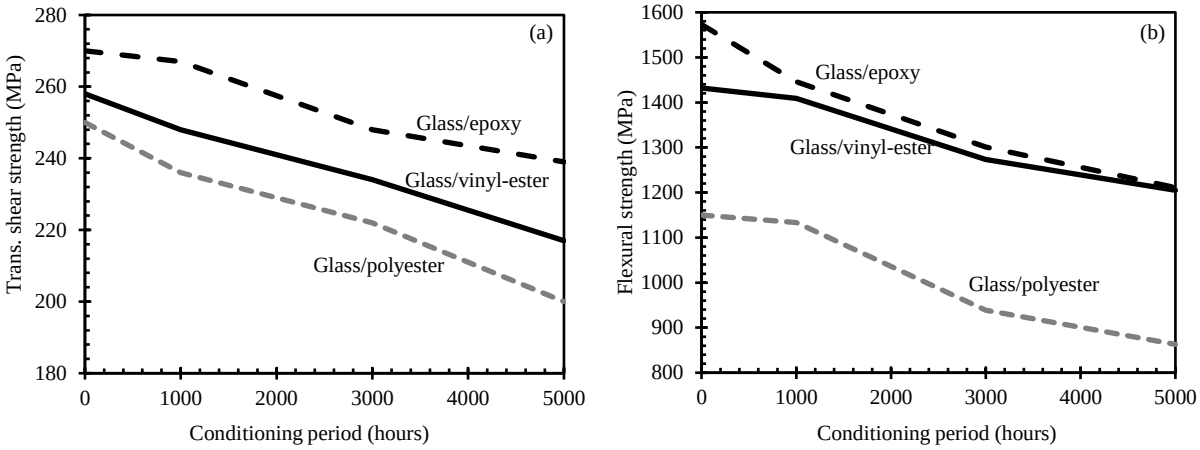

750

751 (a) transverse-shear strength (b) flexural strength

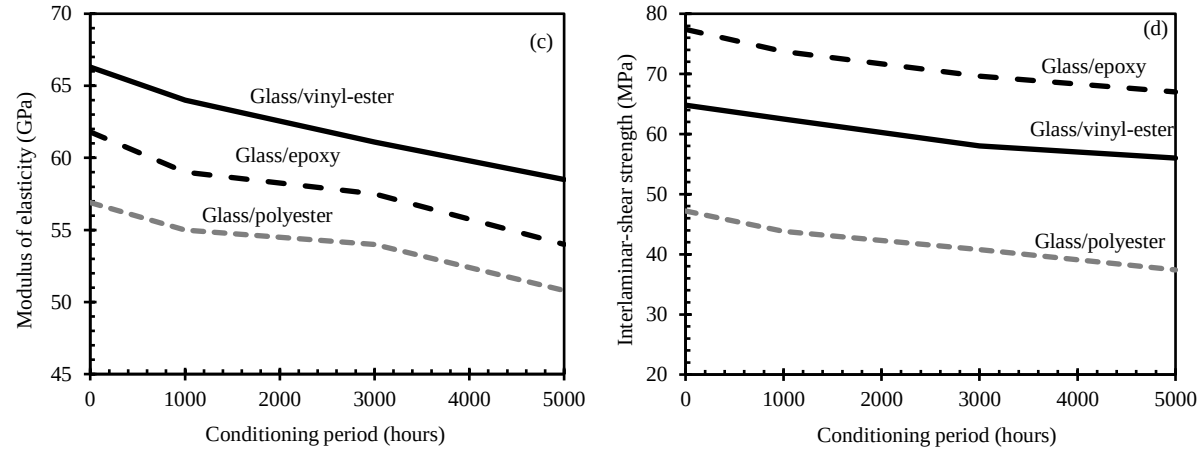

752

753 (c) flexural modulus of elasticity (d) interlaminar-shear strength

754 **Figure 6**. Effect of conditioning in the alkaline solution at 60°C on mechanical properties:

755

756

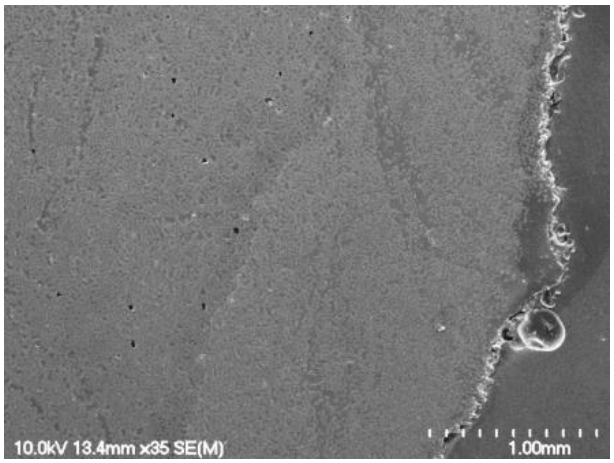

(a) Polyester GFRP bar

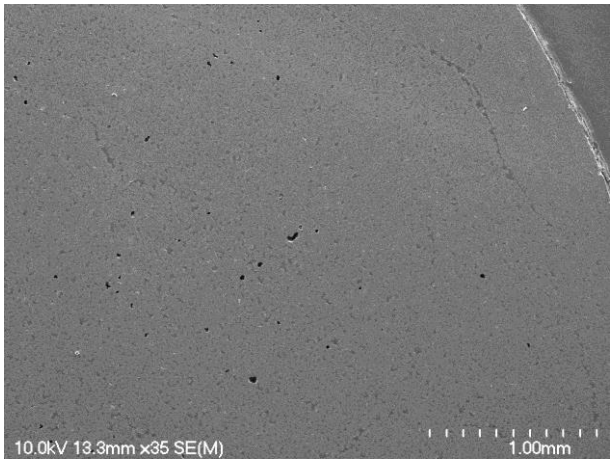

(b) Vinyl-ester GFRP bar

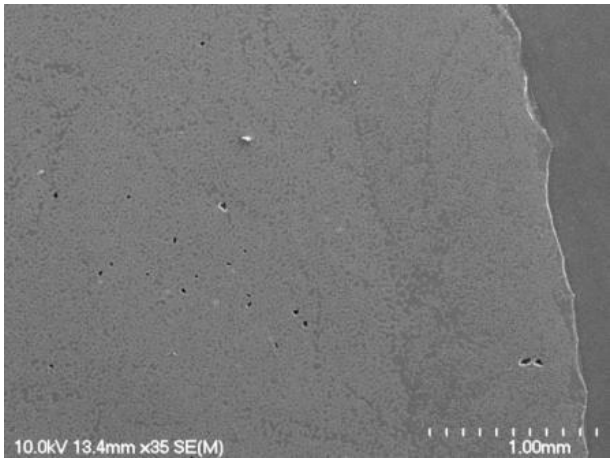

(c) Epoxy GFRP bar

Figure 7. Micrographs of the cross section of the reference GFRP bars

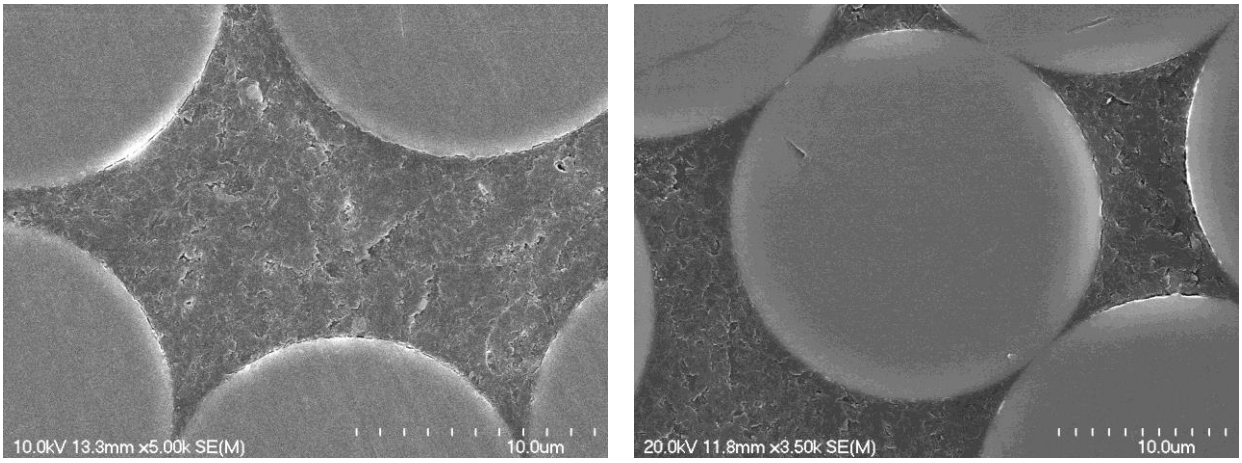

(a) (b)

Figure 8. Micrographs of the fiber–matrix interface of an epoxy GFRP bar before and after conditioning: (a) before conditioning; (b) after conditioning

781 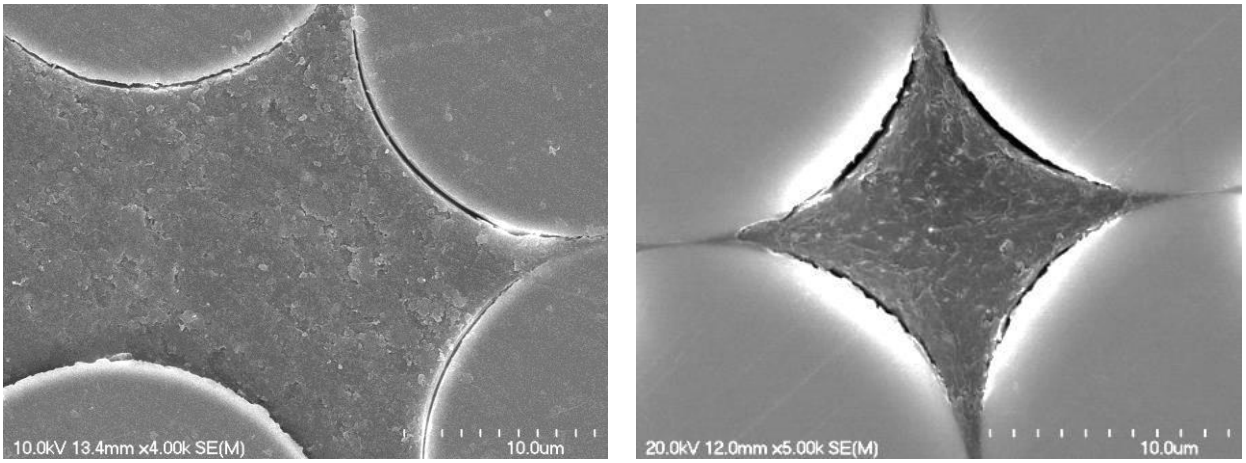

782 (a) (b)

783 **Figure 9**. Micrographs of the fiber–matrix interface of a polyester GFRP bar before and after
784 conditioning: (a) before conditioning; (b) after conditioning

785

786 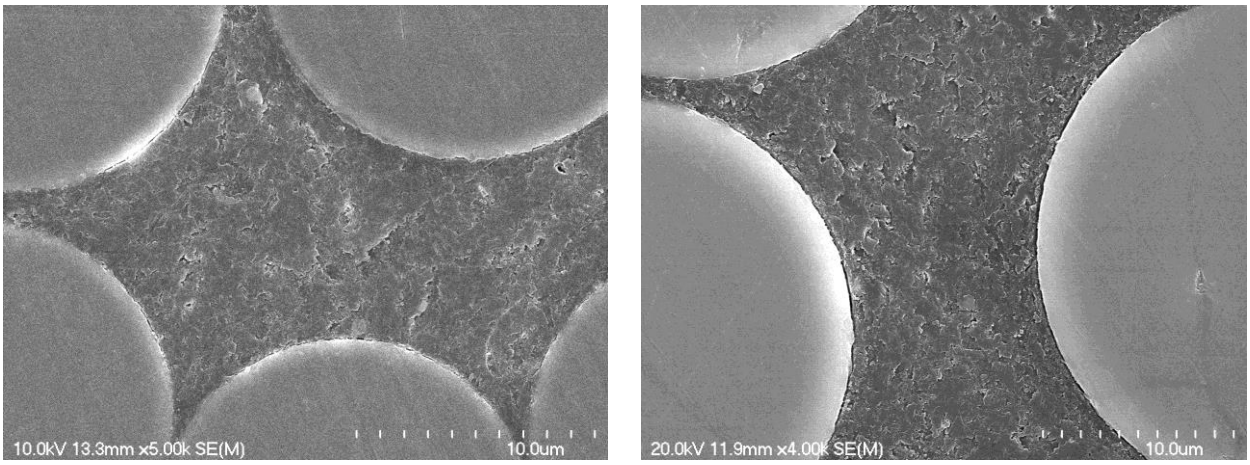

787 (a) (b)

788 **Figure 10**. Micrographs of the fiber/matrix interface of a vinyl-ester GFRP bar before and after
789 conditioning: (a) before conditioning; (b) after conditioning

790

791

792

793

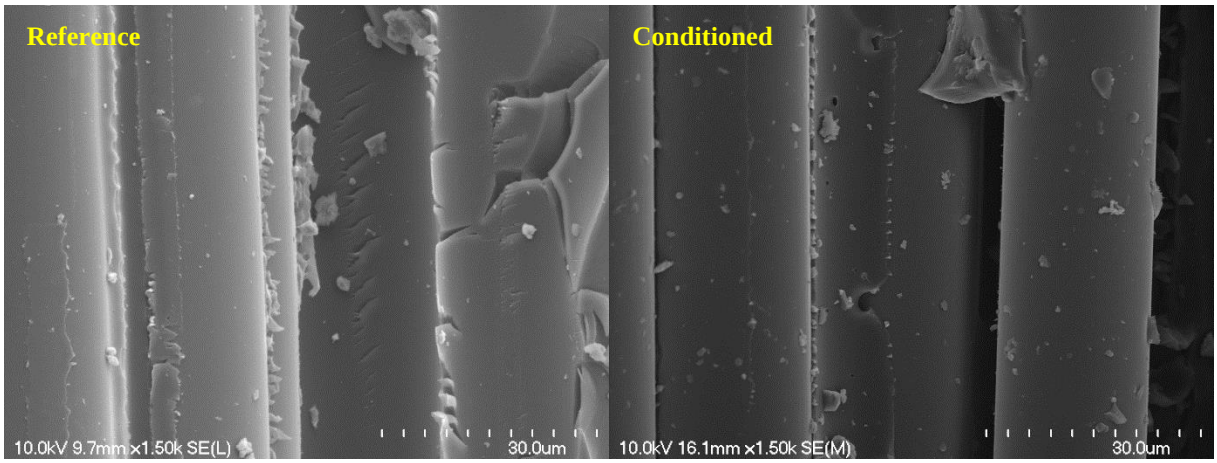

(a)

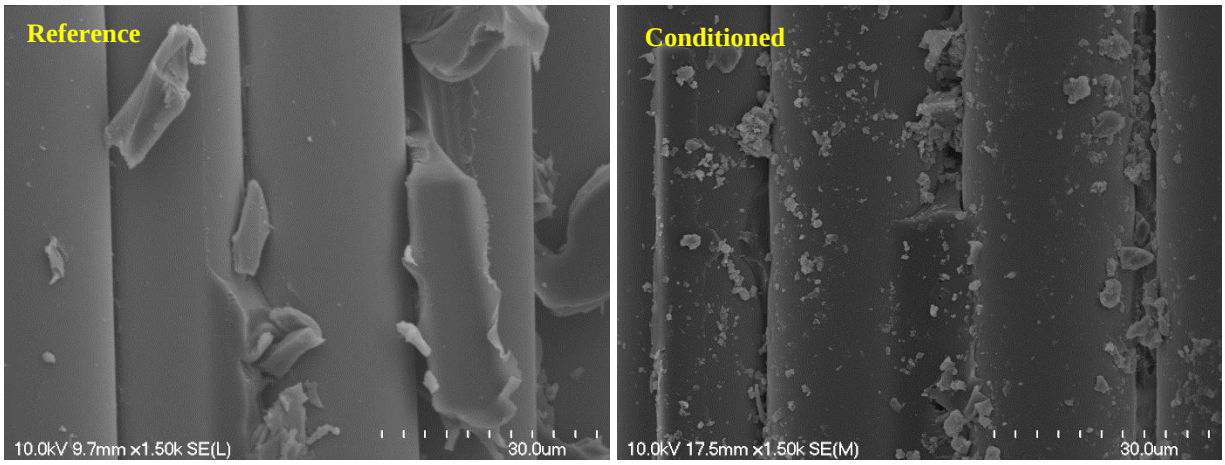

(b)

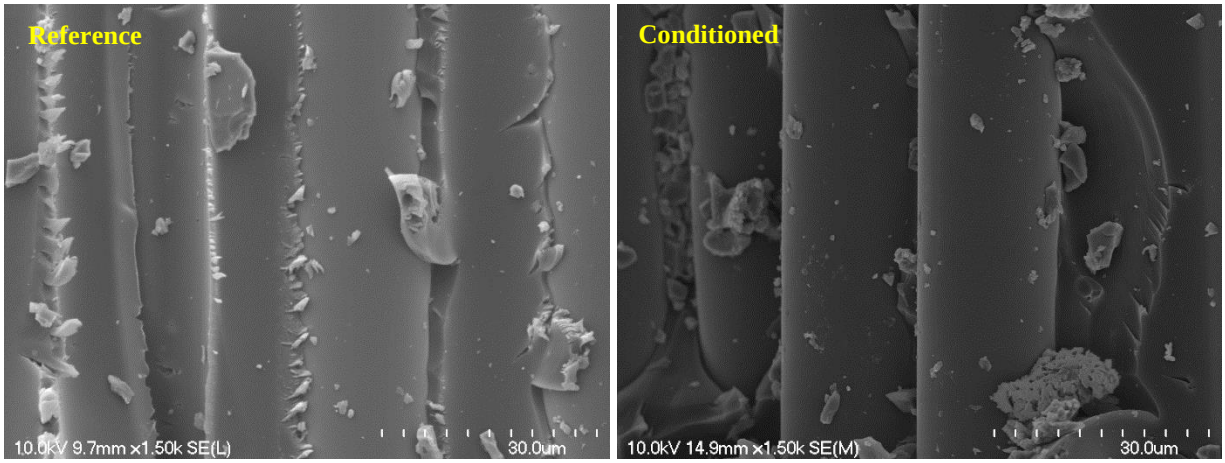

(c)

Figure 11. Micrographs of bars conditioned in the alkaline solution for 1,000 h at 60ºC (after interlaminar shear failure): (a) polyester GFRP; (b) vinyl-ester GFRP; (c) epoxy GFRP

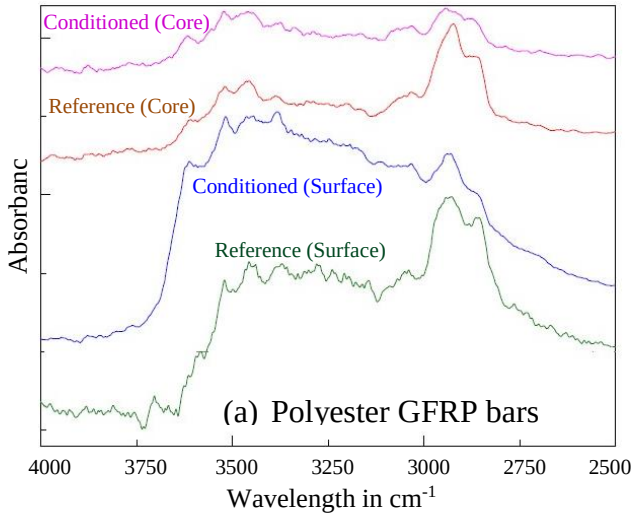

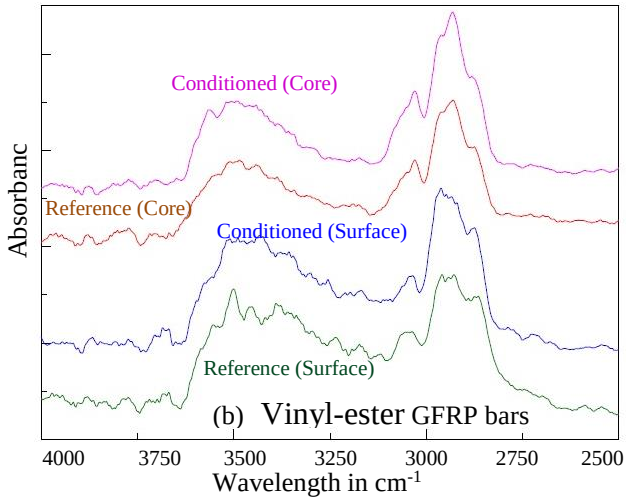

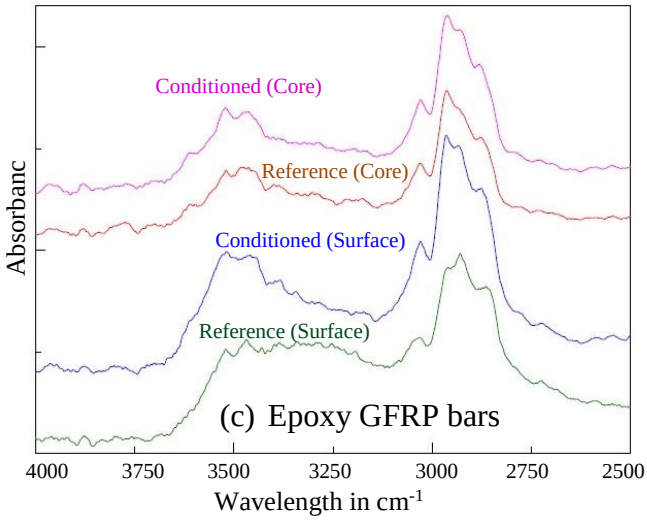

Figure 12. FTIR spectra of reference and specimens conditioned for 5,000 h

809

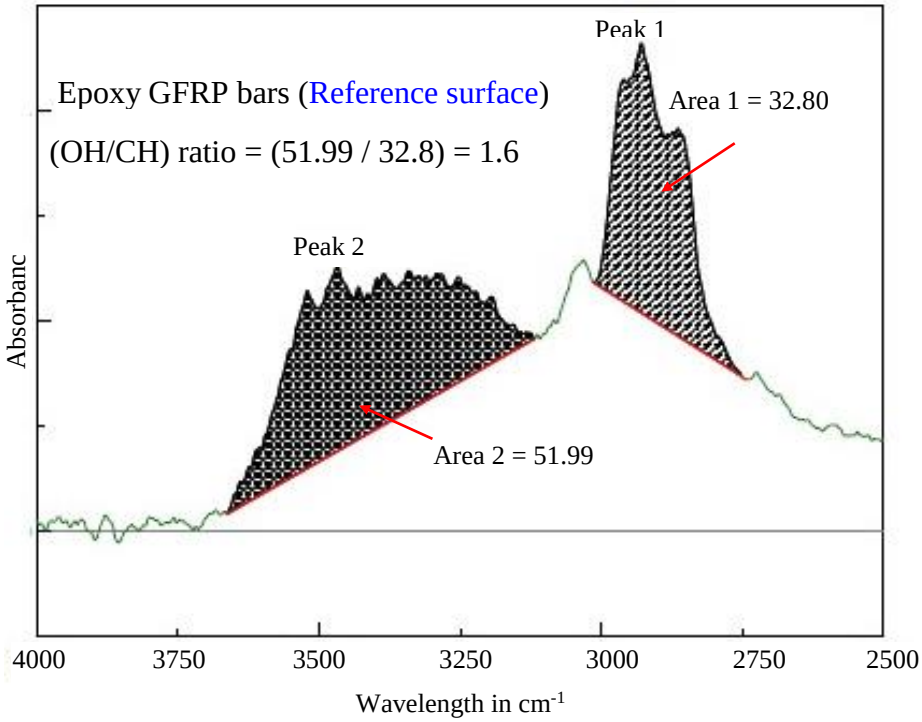

810

811 **Figure 13.** Peak areas used to calculate a O–H/C–H

812